Fröhlich electron-phonon interaction Hamiltonian in a quantum dot quantum well

Li Zhang*
Department of Mechanism and Electron, Panyu Polytechnic, Panyu, 511483, People's Republic of China and Department of Physics, Guihuagang Campus, Guangzhou University, Guangzhou 510405, China

Hong-Jing Xie
Department of Physics, Guihuagang Campus, Guangzhou University, Guangzhou 510405, China

Chuan-Yu Chen
Department of Physics, Guihuagang Campus, Guangzhou University, Guangzhou 510405, China
(Received 23 May 2002; revised manuscript received 29 July 2002; published 27 November 2002)

The phonon modes of a quantum dot quantum well (QDQW) in the nonpolar dielectric surrounding medium are deduced by using the dielectric continuum model. The confined longitudinal-optical (LO) phonon modes both in the core material (LO1) and in the shell material (LO2), interface optical (IO) and surface optical (SO) phonon modes, as well as the corresponding Fröhlich electron-phonon interaction Hamiltonians are derived. A proper eigenfunction for LO1 modes is adopted and a legitimate eigenfunction for LO2 modes is constructed to describe the vibrating of the LO phonons. Numerical calculations are performed on a HgS/CdS QDQW, and the results reveal that there are three branches of IO or SO phonon frequencies in the system. With increasing quantum number *l*, the frequencies of two branches approach those in the single HgS/CdS heterostructure and the reason for this feature is explained. Bigger *l* and a thicker spherical shell make the potentials of IO or SO phonon modes more localized at a certain interface or surface. The study also reveals that the electron-SO phonon coupling is more significant.

DOI: 10.1103/PhysRevB.66.205326 PACS number(s): 71.38.−k, 63.20.Kr, 74.25.Kc

I. INTRODUCTION

Due to the great progress in semiconductor nanotechnology, various kinds of semiconductor heterostructures can be fabricated. Among these, a synthesized inhomogeneous spherical quantum dot with a central core and many layers of shells called a quantum dot quantum well[1–3] (QDQW), formed by by using the wet chemical synthesis method, is a field of great interest to many authors.[4–9] It is well known that the electron-phonon interaction is an important factor influencing the physical properties of polar crystals such as the binding energy of impurities, carrier transportation, and linear and nonlinear optical properties, especially in low-dimensional quantum systems.[10–13] Furthermore, the effect of such an influence becomes stronger as the dimensionality of the system reduces.[14,15] Hence, a proper description of polar optical phonon modes and the electron-phonon interaction Hamiltonian is necessary.

In much previous research on the electron-phonon interaction in a quantum dot (QD), the bulk phonon modes were employed.[15–17] In fact, in the low-dimensional quantum systems, phonons in the polar crystals are confined, which makes the phonon modes more complicated than those in the bulk materials.[18] After the pioneering works of Fuchs and Kliewer[19] and Licari and Evard,[20] Wendler and Haupt[21,22] presented a complete theory of long-wavelength optical phonons and polar-type electron-phonon interaction for any confined systems within the framework of the standard dielectric continuum (DC). Thereafter, under DC approximation, several authors made their contributions to the study of the phonon modes in various quantum systems. Mori and Ando[23] studied the phonon modes in a quantum well (QW) and provided the optical-phonon modes and electron-phonon interaction Hamiltonian. and Shao-hua Jun-jie[24] derived the free optical-phonon modes in the coupled QWs with five layers of heterostructures. Recently, Xie *et al.* studied the phonon modes in a cylindrical quantum well wire (QWW) in a infinite potential boundary condition[12] and a finite potential boundary condition.[11] Klimin *et al.*[25] determined the vibrational modes of inertial polarization in the multilayer QWW and QD. Li and Chen[26] obtained the longitudinal-optical (LO) phonon modes and two types of surface optical (SO) phonon modes of a free-standing cylindrical QD. Klein *et al.*[27] and Roca *et al.*[28] derived the polar optical-phonon modes in a spherical QD. de la Cruz *et al.*[29] dervied the interface optical (IO) phonon modes in a $GaAs/Al_xGa_{1-x}As$ spherical QD, and the interface frequencies as a function of the Al alloy concentration were discussed. Within the framework of the DC model, Tkach *et al.*[30] studied exciton-phonon interaction in a QDQW, and the phonon modes were obtained, but detailed discussions about the characters of phonon modes in the system were missed. Even so, the DC model had its limits in describing optical modes in QW structures, and the region of validity of the approach is limited to the situation in which the phonon wavelengths are large enough as compared with the lattice constant.[24,31–33] It has been proven that the LO and IO phonon modes obtained by the DC model are in good agreement with other calculation approaches.[33–35] Because of the simplicity and efficiency of DC models, especially for polaron effects,[11,12] in the present paper, we will use them to study the phonon modes and the electron-phonon interaction in a QDQW.

The semiconductor materials usually used to synthesize QDQW's are CdS/HgS, ZnSe/CdSe, CdS/PbS, etc.[1–9] The

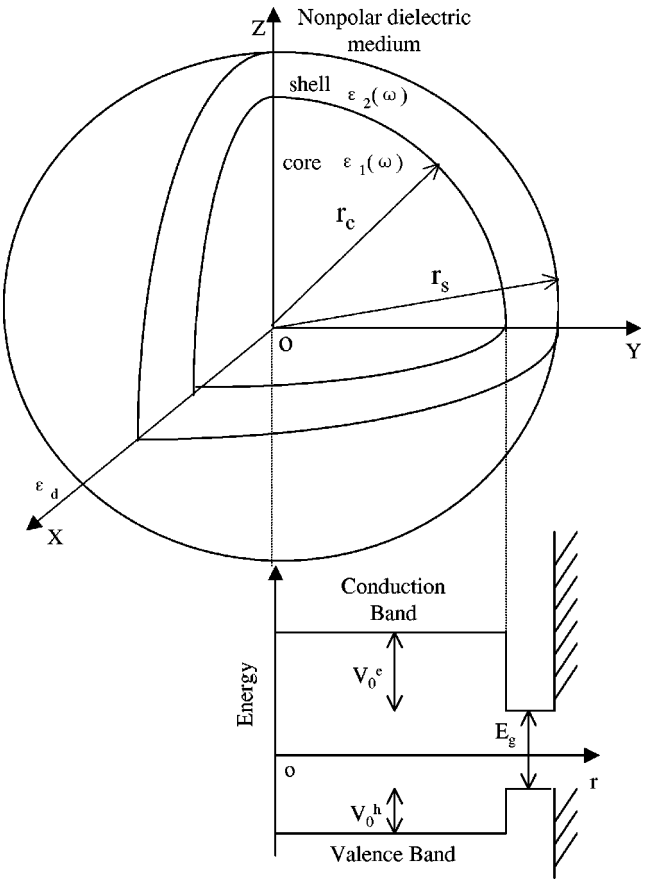

FIG. 1. Schematic view of our model of the QDQW and corresponding potential profile. $\varepsilon_1(\omega)$, $\varepsilon_2(\omega)$ are the dielectric functions of the core material and shell material, respectively. ε_d is the dielectric constant of the nonpolar dielectric surrounding medium. V_0^e (V_0^h) is the conduction- (valence-) band offset between the core and shell region, while E_g refers to the shell region semiconductor band gap.

material with the smaller bulk band gap (such as HgS) is embedded between a core and an outer shell of the material with a larger bulk band gap (such as CdS), so the material with a smaller bulk band gap acts as a well material for the electron and hole as well as the phonon in the polar crystal.

In this paper, we will consider a QDQW with a central core ($r \leqslant r_c$) and a shell ($r_c < r \leqslant r_s$) in the nonpolar surrounding medium ($r > r_s$) with a dielectric constant ε_d. A schematic view of our simplified model of the QDQW and corresponding radial potential profile are given in Fig. 1. The advantages of this work are that, (i) using the analogy method in Refs. 11 and 12, the works of phonon modes in a cylindrical QWW have been extended to QDQW systems; (ii) the orthonormal relation for the polarization vectors have been derived, and via the relation, the phonon field and the electron-phonon interaction have been quantized, which may be useful for further work, such with polaron effects, bound polaron effects and phonon scattering in the QDQW systems; and (iii) from the discussions of the dispersion relations and the potential distributions for the IO or SO phonon modes, the characters of IO or SO phonon modes have been determined, and the results may be helpful to study and understand the polaronic effect, electron scattering, etc., in the systems. The paper is organized as follows: in Sec. II, two confined LO phonon modes both in the central core (LO1) and in the shell region (LO2), the IO and SO phonon modes, as well as the corresponding Fröhlich electron-phonon interaction Hamiltonians are deduced. In Sec. III, numerical calculations on a HgS/CdS QDQW are performed, and the characters of the IO and SO phonon modes are discussed. In the last section, a brief summary about characters of the phonon modes and the applied range of this theory are discussed and specified.

II. THEORY

Under the DC approximation, and starting from the classic electrostatics equations for free oscillation [$\rho_0(\mathbf{r})=0$], we have

$$\varepsilon \nabla^2 \phi(\mathbf{r}) = 0 \tag{1}$$

with

$$\varepsilon(\omega) = \varepsilon_\infty + \frac{\varepsilon_0 - \varepsilon_\infty}{1 - \omega^2/\omega_{TO}^2}, \tag{2}$$

where ε_0, ε_∞ are the static and high-frequency dielectric constants, respectively, and ω_{TO} is the frequency of transverse-optical phonon.

A. The confined LO phonon modes

There are two possible solutions for Eq. (1): one is $\varepsilon(\omega)=0$, and the other is $\nabla^2\phi(\mathbf{r})=0$. To the first solution, via Eq. (2) and a Lyddane-Sachs-Teller (LST) relation, one can get

$$\omega^2 = \omega_{TO}^2 \frac{\varepsilon_0}{\varepsilon_\infty} = \omega_{LO}^2, \tag{3}$$

which describes the confined bulk LO modes of frequency $\omega = \omega_{LO}$, where ω_{LO} is the frequency of a LO phonon.

1. Confined LO1 modes in the core

The eigenfunctions for the confined LO1 mode inside the core region ($r \leqslant r_c$) can be chosen as

$$\phi_{lmn}^{LO1}(\mathbf{r}) = \begin{cases} C_{ln} j_l\left(\dfrac{\alpha_{ln}}{r_c} r\right) Y_{lm}(\theta,\varphi) & r \leqslant r_c, \\ 0 & r > r_c, \end{cases} \tag{4}$$

where $j_l(x)$ is the spherical Bessel function of the lth order, Y_{lm} is the spherical harmonics, and α_{ln} is the nth zero of $j_l(x)$. It should be noted that, in the region outside the core ($r \leqslant r_c$), the eigenfunctions should be zero, which are the demands of the continuum of electric field and electric displacement at the boundary.[11,12,20]

Using the same steps as in Ref. 11, we obtain the confined LO1 phonon Hamiltonian as

$$H_{LO1}=\frac{1}{2}\int\left[n^*\mu\left(\frac{1+\frac{8}{3}\pi n^*\alpha}{n^*e}\right)^2\dot{\mathbf{P}}^*\cdot\dot{\mathbf{P}}+n^*\mu\omega_{LO1}^2\left(\frac{1+\frac{8}{3}\pi n^*\alpha}{n^*e}\right)^2\mathbf{P}^*\cdot\mathbf{P}\right]\mathrm{d}^3\mathbf{r}, \quad (5)$$

where μ is the reduced mass of the ion pair, n^* is the number of ion pairs per unit volume, α is the electronic polarizability per ion pair, and $\mathbf{P}$ is the polarization vector.

Via the Green's first identity, it is easy to get the orthonormal relation for the polarization vectors $\mathbf{P}_{lmn}^{LO1}$,

$$\begin{aligned}\int\mathbf{P}_{l'm'n'}^{LO1*}\cdot\mathbf{P}_{lmn}^{LO1}\mathrm{d}^3\mathbf{r}&=\frac{1}{16\pi^2}\int\nabla\phi_{l'm'n'}^{LO1}\cdot\nabla\phi_{lmn}^{LO1}\mathrm{d}^3\mathbf{r}\\&=-\frac{1}{16\pi^2}\int\phi_{l'm'n'}^{LO1},\nabla^2\phi_{lmn}^{LO1}\mathrm{d}^3\mathbf{r}\\&=\frac{|C_{ln}|^2\alpha_{ln}^2r_c}{32\pi^2}j_{l+1}^2(\alpha_{ln})\delta_{l'l}\delta_{m'm}\delta_{n'n}.\end{aligned} \quad (6)$$

If we choose C_{ln} to be

$$C_{ln}=\left[\frac{1}{n^*\mu}\left(\frac{n^*e}{1+\frac{8}{3}\pi n^*\alpha}\right)^2\frac{16\pi^2}{\alpha_{ln}^2r_cj_{l+1}(\alpha_{ln})^2}\right]^{1/2}, \quad (7)$$

then $\mathbf{P}_{lmn}^{LO1}$ may form an orthonormal and complete set. We introduce creation and annihilation operators $a_{lmn}^\dagger$ and a_{lmn} to express the polarization vector $\mathbf{P}$ and the standard Hamiltonian H_{LO1}:

$$\mathbf{P}=\sum_{lmn}\left(\frac{\hbar}{\omega_{LO1}}\right)^{1/2}[a_{lmn}^\dagger+a_{lmn}]\mathbf{P}_{lmn}^{LO1}, \quad (8)$$

$$\dot{\mathbf{P}}=-i\sum_{lmn}(\hbar\omega_{LO1})^{1/2}[a_{lmn}^\dagger-a_{lmn}]\mathbf{P}_{lmn}^{LO1}, \quad (9)$$

$$H_{LO1}=\sum_{lmn}\hbar\omega_{LO1}[a_{lmn}^\dagger a_{lmn}+\tfrac{1}{2}]. \quad (10)$$

The operators for the LO1 phonon of the lmn satisfy the commutation relation for bosons. The eigenfunction of the LO1 phonon modes $\phi(\mathbf{r})$ could be expanded in terms of the normal modes, so the Fröhlich Hamiltonian between the electron and LO1 phonon is obtained as

$$\begin{aligned}H_{e-LO1}&=-e\phi^{LO1}(\mathbf{r})\\&=-\sum_{lmn}\left[\Gamma_{ln}^{LO1}j_l\left(\frac{\alpha_{ln}}{r_c}r\right)Y_{lm}(\theta,\varphi)a_{lmn}^\dagger+\mathrm{H.c.}\right],\end{aligned} \quad (11)$$

where

$$\begin{aligned}|\Gamma_{ln}^{LO1}|^2&=\frac{1}{n^*\mu\omega_{LO1}}\left(\frac{n^*e}{1+\frac{8}{3}\pi n^*\alpha}\right)^2\frac{16\pi^2e^2\hbar}{\alpha_{ln}^2r_cj_{l+1}^2(\alpha_{ln})}\\&=\frac{4\pi e^2\hbar\omega_{LO1}}{\alpha_{ln}^2r_cj_{l+1}^2(\alpha_{ln})}\left(\frac{1}{\varepsilon_{1\infty}}-\frac{1}{\varepsilon_{10}}\right).\end{aligned} \quad (12)$$

2. Confined LO2 modes in the shell region

The potential for the LO2 phonon modes in the shell region ($r_c\leqslant r\leqslant r_s$) can be chosen as

$$\phi_{lmn}^{LO2}(\mathbf{r})=\begin{cases}B_{ln}T_l\left(\frac{a_{ln}}{r_c}r\right)Y_{lm}(\theta,\varphi) & r_c\leqslant r\leqslant r_s,\\ 0 & \text{otherwise},\end{cases} \quad (13)$$

where

$$T_l\left(\frac{a_{ln}}{r_c}r\right)=j_l\left(\frac{a_{ln}}{r_c}r\right)+b_{ln}n_l\left(\frac{a_{ln}}{r_c}r\right), \quad (14)$$

and $n_l(x)$ is the spherical Neumann function of order l. $T_l(a_{ln}r/r_c)$ satisfies the boundary conditions at $r=r_c$ and $r=r_s$. They are

$$\begin{aligned}T_l\left(\frac{a_{ln}}{r_c}r\right)\Big|_{r=r_c}&=j_l(a_{ln})+b_{ln}n_l(a_{ln})=0,\\T_l\left(\frac{a_{ln}}{r_c}r\right)\Big|_{r=r_s}&=j_l\left(\frac{a_{ln}}{r_c}r_s\right)+b_{ln}n_l\left(\frac{a_{ln}}{r_c}r_s\right)=0,\end{aligned} \quad (15)$$

so a_{ln} and b_{ln} can be solved using Eq. (15). n in the radial function $T_l(a_{ln}r/r_c)$ denotes the number of zeros within the range of $r_c\leqslant r\leqslant r_s$. By using the spherical Bessel equation, it can be proved that $T_l(a_{ln}r/r_c)$ and $T_l(a_{lm}r/r_c)$ are orthogonalized in the shell region (refer to the appendix).

Similar to the process for LO1, we obtained the following orthogonal relation of polarization vector $\mathbf{P}_{lmn}^{LO2}$:

$$\begin{aligned}&\int\mathbf{P}_{l'm'n'}^{LO2*}\cdot\mathbf{P}_{lmn}^{LO2}\mathrm{d}^3\mathbf{r}\\&=\frac{1}{16\pi^2}\int\nabla\phi_{l'm'n'}^{LO2}\cdot\nabla\phi_{lmn}^{LO2}\mathrm{d}^3\mathbf{r}\\&=-\frac{1}{16\pi^2}\int\phi_{l'm'n'}^{LO2},\nabla^2\phi_{lmn}^{LO2}\mathrm{d}^3\mathbf{r}\\&=\frac{a_{ln}^2|B_{ln}|^2}{32\pi^2r_c^2}\left\{r^3\left[T_l\left(\frac{a_{ln}}{r_c}r\right)^2-T_{l-1}\left(\frac{a_{ln}}{r_c}r\right)T_{l+1}\left(\frac{a_{ln}}{r_c}r\right)\right]\right\}_{r_c}^{r_s}\delta_{l'l}\delta_{m'm}\delta_{n'n}\\&=\frac{a_{ln}^2|B_{ln}|^2r_c}{32\pi^2}[T_{l-1}(a_{ln})T_{l+1}(a_{ln})\end{aligned}$$

$$-\gamma^3 T_{l-1}(\gamma a_{ln}) T_{l+1}(\gamma a_{ln})]\delta_{l'l}\delta_{m'm}\delta_{n'n}, \tag{16}$$

where

$$\gamma = r_s/r_c. \tag{17}$$

We let

$$|B_{ln}|^2 = \frac{16\pi^2}{n^*\mu a_{ln}^2 r_c}\left(\frac{n^* e}{1+\frac{8}{3}\pi n^*\alpha}\right)^2 [T_{l-1}(a_{ln})T_{l+1}(a_{ln}) - \gamma^3 T_{l-1}(\gamma a_{ln})T_{l+1}(\gamma a_{ln})]^{-1}, \tag{18}$$

so $\mathbf{P}_{lmn}^{LO2}$ forms an orthonormal and complete set, which could be used to express H_{LO2} and $H_{e\text{-}LO2}$ as the following

$$H_{LO2} = \sum_{lmn} \hbar\omega_{LO2}[b_{lmn}^\dagger b_{lmn} + \tfrac{1}{2}], \tag{19}$$

$$H_{e\text{-}LO2} = -e\phi^{LO2}(\mathbf{r}) = -\sum_{lmn}\left[\Gamma_{ln}^{LO2} T_l\left(\frac{a_{ln}}{r_c}r\right) Y_{lm}(\theta,\varphi) b_{lmn}^\dagger + \text{H.c.}\right] \tag{20}$$

with

$$|\Gamma_{ln}^{LO2}|^2 = \frac{4\pi e^2\hbar\omega_{LO2}}{a_{ln}^2 r_c}[T_{l-1}(a_{ln})T_{l+1}(a_{ln}) - \gamma^3 T_{l-1}(\gamma a_{ln})T_{l+1}(\gamma a_{ln})]^{-1}\left(\frac{1}{\varepsilon_{2\infty}} - \frac{1}{\varepsilon_{20}}\right), \tag{21}$$

where $b_{lmn}^\dagger$ and b_{lmn} are the Bose creation and annihilation operations for the LO2 phonon of the lmn mode.

B. The IO and SO phonon modes

The second possible solution of electrostatic Eq. (1) is Laplace equation, and it will give the interface phonon and surface phonon modes. Following Eq. (5), we get the Hamiltonian for the IO phonon or the SO phonon[11,12]

$$H_{\text{IO, SO}} = \frac{1}{2}\int\left(n^*\mu\left\{\frac{1}{n^* e[1+(\alpha\mu/e^2)(\omega_0^2-\omega^2)]}\right\}^2 \dot{\mathbf{P}}^*\cdot\dot{\mathbf{P}} + n^*\mu\omega^2\left\{\frac{1}{n^* e[1+(\alpha\mu/e^2)(\omega_0^2-\omega^2)]}\right\}^2 \times \mathbf{P}^*\cdot\mathbf{P}\right)\mathrm{d}^3\mathbf{r}. \tag{22}$$

It is understood that IO and SO phonon modes belong to the whole system,[25,30] especially, in the QDQW system in which the shell width is relatively thin, so the IO and SO modes are coupled on each interface or surface. For the IO and SO phonon modes, under the spherical coordinate, the solution of Laplace equation is written as

$$\phi_{lm}^{IO,SO}(\mathbf{r}) = \begin{cases} \left(\frac{1}{r_s}\gamma^{-l} - \frac{1}{r_c}\gamma^l\right) A_l r^l Y_{lm}(\theta,\varphi) & r \le r_c, \\ \left[\left(\frac{1}{r_s}\gamma^{-l}A_l - \beta^{-l-1}D_l\right)r^l + \left(\frac{1}{r_s}\gamma^{-l}D_l - \beta^l A_l\right)r^{-l-1}\right] Y_{lm}(\theta,\varphi) & r_c < r \le r_s, \\ \left(\frac{1}{r_s}\gamma^{-l} - \frac{1}{r_c}\gamma^l\right) D_l r^{-l-1} Y_{lm}(\theta,\varphi) & r > r_s, \end{cases} \tag{23}$$

where γ is defined in Eq. (17) and $\beta = r_c \cdot r_s$, in which the continuity of the eigenfunction at $r = r_c$, r_s has been taken into consideration.

Other than the LO phonon, the dielectric functions $\varepsilon(\omega)$ of the IO or SO phonons do not equal and zero, they are given by Eq. (2) and the LST relations

$$\varepsilon_1(\omega) = \varepsilon_{1\infty}\frac{\omega^2-\omega_{LO1}^2}{\omega^2-\omega_{TO1}^2}, \quad \varepsilon_2(\omega) = \varepsilon_{2\infty}\frac{\omega^2-\omega_{LO2}^2}{\omega^2-\omega_{TO2}^2}. \tag{24}$$

The boundary conditions at $r = r_c$ and r_s imply

$$\varepsilon_1(\omega)\frac{\partial\phi_{1lm}}{\partial r}\bigg|_{r=r_c} = \varepsilon_2(\omega)\frac{\partial\phi_{2lm}}{\partial r}\bigg|_{r=r_c}, \tag{25}$$

$$\varepsilon_2(\omega)\frac{\partial\phi_{2lm}}{\partial r}\bigg|_{r=r_s} = \varepsilon_d\frac{\partial\phi_{3lm}}{\partial r}\bigg|_{r=r_s}. \tag{26}$$

Substituting Eq. (23) into Eqs. (25) and (26), we get the following linear homogeneous equations for A_l and D_l:

$$\left(\frac{1}{r_s}\gamma^{-l} - \frac{1}{r_c}\gamma^l\right) l r_c^{l-1} A_l \varepsilon_1(\omega) = \left(\frac{1}{r_s}\gamma^{-l}A_l - \beta^{-l-1}D_l\right) l r_c^{l-1}\varepsilon_2(\omega) - \left(\frac{1}{r_s}\gamma^{-l}D_l - \beta^l A_l\right)(l+1) r_c^{-l-2}\varepsilon_2(\omega), \tag{27}$$

$$\left(\frac{1}{r_s}\gamma^{-l} - \frac{1}{r_c}\gamma^l\right)(-l-1) r_s^{-l-2} D_l \varepsilon_d = \left(\frac{1}{r_s}\gamma^{-l}A_l - \beta^{-l-1}D_l\right) l r_s^{l-1}\varepsilon_2(\omega) - \left(\frac{1}{r_s}\gamma^{-l}D_l - \beta^l A_l\right)(l+1) r_s^{-l-2}\varepsilon_2(\omega). \tag{28}$$

To obtain the nonzero solutions for A_l and D_l, the following secular equation should be satisfied.

$$\begin{vmatrix} \left(\frac{1}{r_s}\gamma^{-l}-\frac{1}{r_c}\gamma^{l}\right) l r_c^{l-1}\varepsilon_1 & \left[\beta^{-l-1} l r_c^{l-1}+\frac{1}{r_s}\gamma^{-l}(l+1)r_c^{-l-2}\right]\varepsilon_2 \\ \quad -[\gamma^{-l-1} l r_c^{l-2}+\beta^{l}(l+1)r_c^{-l-2}]\varepsilon_2 & \\ \left[\frac{1}{r_s}\gamma^{-l} l r_s^{l-1}+\beta^{l}(l+1)r_s^{-l-2}\right]\varepsilon_2 & [-\beta^{-l-1} l r_s^{l-1}-\gamma^{-l}(l+1)r_s^{-l-3}]\varepsilon_2 \\ & \quad +\left(\frac{1}{r_s}\gamma^{-l}-\frac{1}{r_c}\gamma^{l}\right)(l+1)r_s^{-l-2}\varepsilon_d \end{vmatrix} = 0. \tag{29}$$

Equation (29) gives the dispersion relations for IO and SO phonons. Substituting Eq. (24) into Eq. (29), above the frequencies of the IO and SO phonons can be derived by solving the sixth-order equation for ω. When ω is worked out, it is easy to get the values of $\varepsilon_1(\omega)$ and $\varepsilon_2(\omega)$ via Eq. (24). Through Eq. (27) or (28), the relation of A_l and D_l can be expressed as

$$D_l = f_l(\omega) A_l, \tag{30}$$

where

$$f_l(\omega) = -\frac{(\gamma^{-l-1}-\gamma^{l}) l r_c^{l-2}\varepsilon_1 - \gamma^{-l-1} l r_c^{l-2}\varepsilon_2 - \beta^{l}(l+1)r_c^{-l-2}\varepsilon_2}{\beta^{-l-1} l r_c^{l-1}\varepsilon_2 + \gamma^{-l-1}(l+1)r_c^{-l-3}\varepsilon_2} \tag{31}$$

or

$$f_l(\omega) = -\frac{\gamma^{-l} l r_s^{l-2}\varepsilon_2 + \beta^{l}(l+1)r_s^{-l-2}\varepsilon_2}{-\beta^{-l-1} l r_s^{l-1}\varepsilon_2 - \gamma^{-l}(l+1)r_s^{-l-3}\varepsilon_2 + (\gamma^{-l}-\gamma^{l+1})(l+1)r_s^{-l-3}\varepsilon_d}. \tag{32}$$

Using the formula (30), the potential functions (23) of the IO and SO phonons can be rewritten as

$$\phi_{lm}^{IO,SO}(\mathbf{r}) = \begin{cases} A_l\left(\frac{1}{r_s}\gamma^{-l}-\frac{1}{r_c}\gamma^{l}\right) r^{l} Y_{lm}(\theta,\varphi) & r \leqslant r_c, \\ A_l\left[\left(\frac{1}{r_s}\gamma^{-l}-\beta^{-l-1}f_l(\omega)\right) r^{l}\right. & \\ \quad \left.+\left(\frac{1}{r_s}\gamma^{-l}f_l(\omega)-\beta^{l}\right) r^{-l-1} Y_{lm}(\theta,\varphi)\right. & r_c < r \leqslant r_s, \\ A_l\left(\frac{1}{r_s}\gamma^{-l}-\frac{1}{r_c}\gamma^{l}\right) f_l(\omega) r^{-l-1} Y_{lm}(\theta,\varphi), & r > r_s. \end{cases} \tag{33}$$

The polarization fields for the IO and SO phonon modes of the QDQW are expressed as

$$\mathbf{P}_{lm}^{IO,SO} = A_l \frac{1-\varepsilon(\omega)}{4\pi}\nabla\phi_{lm}^{IO,SO}(\mathbf{r}). \tag{34}$$

The orthogonal relation for $\mathbf{P}_{lm}^{IO,SO}$ is derived by

$$\begin{aligned} &\int \mathbf{P}_{l'm'}^{IO,SO*}\cdot\mathbf{P}_{lm}^{IO,SO}\mathrm{d}^3\mathbf{r} \\ &= \frac{(1-\varepsilon_1)^2}{16\pi^2}\int_{V1}\nabla\phi_{1l'm'}^{*}\cdot\nabla\phi_{1lm}\mathrm{d}^3\mathbf{r} \\ &\quad + \frac{(1-\varepsilon_2)^2}{16\pi^2}\int_{V2}\nabla\phi_{2l'm'}^{*}\cdot\nabla\phi_{2lm}\mathrm{d}^3\mathbf{r} \\ &= \frac{(1-\varepsilon_1)^2}{16\pi^2}\int_{S1}\phi_{1l'm'}\frac{\partial\phi_{1lm}}{\partial\mathrm{n}}\mathrm{d}a \\ &\quad + \frac{(1-\varepsilon_2)^2}{16\pi^2}\int_{S1+S2}\phi_{2l'm'}\frac{\partial\phi_{2lm}}{\partial\mathrm{n}}\mathrm{d}a \\ &= \frac{|A_l|^2}{16\pi^2}\left\{(1-\varepsilon_1)^2 l\left((\gamma^{-l-1}-\gamma^{l})^2 r_c^{2l-1}\right.\right. \\ &\quad + (1-\varepsilon_2)^2\left\{ l\left[\frac{1}{r_s}\gamma^{-l}-\beta^{-l-1}f_l(\omega)\right]^2\right. \\ &\quad \times(\gamma^{2l+1}-1)r_c^{2l+1} - (l+1) \\ &\quad \left.\left.\left.\times\left[\frac{1}{r_s}\gamma^{-l}f_l(\omega)-\beta^{l}\right]^2(\gamma^{-2l-1}-1)r_c^{-2l-1}\right\}\right) \\ &\quad \times\delta_{l'l}\delta_{m'm}. \end{aligned} \tag{35}$$

TABLE I. The material parameters (Ref. 30) (m_0 is the bare electron mass).

Material	m^*/m_0	$\hbar\omega_{\mathrm{LO}}$ (meV)	ε_0	ε_∞
CdS	0.2	57.2	9.1	5.5
HgS	0.036	27.8	18.2	11.36
H_20	1		1.78	1.78

To choose A_l as

$$|A_l|^{-2}=\frac{1}{2\pi\omega^2}\left(\left(\frac{1}{\varepsilon_1-\varepsilon_{10}}-\frac{1}{\varepsilon_1-\varepsilon_{1\infty}}\right)^{-1} l(\gamma^{-l-1}-\gamma^l)^2 r_c^{2l-1}+\left\{ l\left[\frac{\gamma^{-l}}{r_s}-\beta^{-l-1}f_l(\omega)\right]^2(\gamma^{2l+1}-1)r_c^{2l+1}-(l+1)\left[\frac{1}{r_s}\gamma^{-l}f_l(\omega)-\beta^l\right]^2(\gamma^{-2l-1}-1)r_c^{-2l-1}\right\}\left(\frac{1}{\varepsilon_2-\varepsilon_{20}}-\frac{1}{\varepsilon_2-\varepsilon_{2\infty}}\right)^{-1}\right). \tag{36}$$

can make $\mathbf{P}_{lm}^{IO,SO}$ form an orthonormal and complete set. Similarly we have the Hamiltonian operator for the IO and SO phonons as

$$H_{IO,SO}=\sum_{lm}\hbar\omega[c_{lm}^{\dagger}c_{lm}+\tfrac{1}{2}], \tag{37}$$

where $c_{lm}^{\dagger}$ and c_{lm} are creation and annihilation operators for IO and SO phonons of the (l,m)th modes. They satisfy the commutative rules for bosons. The Fröhlich Hamiltonian describing the interaction between the electron and the IO and SO phonon is written as

$$H_{e\text{-}IO,SO}=-\sum_{lm}\Gamma_l^{IO,SO}(r)[Y_{lm}(\theta,\varphi)c_{lm}+\mathrm{H.c.}], \tag{38}$$

where the electron-IO or- SO phonon radial coupling function is

$$\Gamma_l^{IO,SO}(r)=N_l\times\begin{cases}\left(\frac{1}{r_s}\gamma^{-l}-\frac{1}{r_c}\gamma^l\right)r^l & r\leqslant r_c,\\ \left[\left(\frac{1}{r_s}\gamma^{-l}-\beta^{-l-1}f_l(\omega)\right)r^l+\left(\frac{1}{r_s}\gamma^{-l}f_l(\omega)-\beta^l\right)r^{-l-1}\right] & r_c<r\leqslant r_s,\\ \left(\frac{1}{r_s}\gamma^{-l}-\frac{1}{r_c}\gamma^l\right)f_l(\omega)r^{-l-1} & r>r_s\end{cases} \tag{39}$$

with

$$|N_l|^2=|A_l|^2\frac{e^2\hbar}{\omega}=2\pi e^2\hbar\omega\left(\left(\frac{1}{\varepsilon_1-\varepsilon_{10}}-\frac{1}{\varepsilon_1-\varepsilon_{1\infty}}\right)^{-1}\times l(\gamma^{-l-1}-\gamma^l)^2r_c^{2l-1}+\left\{l\left[\frac{\gamma^{-l}}{r_s}-\beta^{-l-1}f_l(\omega)\right]^2(\gamma^{2l+1}-1)r_c^{2l+1}-(l+1)\left[\frac{1}{r_s}\gamma^{-l}f_l(\omega)-\beta^l\right]^2(\gamma^{-2l-1}-1)r_c^{-2l-1}\right\}\times\left(\frac{1}{\varepsilon_2-\varepsilon_{20}}-\frac{1}{\varepsilon_2-\varepsilon_{2\infty}}\right)^{-1}\right)^{-1}. \tag{40}$$

So the total Hamiltonian of the free phonon field in a QDQW should include the two confined bulk LO modes, and the IO and SO mixing phonon modes, i.e.,

$$H_{\mathrm{tot\ ph}}=H_{LO1}+H_{LO2}+H_{IO,SO}, \tag{41}$$

and the total Fröhlich electron-phonon interaction should also include three terms

$$H_{e\text{-}ph}=H_{e\text{-}LO1}+H_{e\text{-}LO2}+H_{e\text{-}IO,SO}, \tag{42}$$

in which H_{LO1}, H_{LO2}, and $H_{IO,SO}$, and $H_{e\text{-}LO1}$, $H_{e\text{-}LO2}$, and $H_{e\text{-}IO,SO}$ are given by EqS. (10), (19), and (37), and (11), (20), and (38) respectively.

III. NUMERICAL RESULTS AND DISCUSSIONS

In order to see more clearly the characters of the phonon modes, numerical calculations on a HgS/CdS QDQW are performed. Due to the simplicity of the electron-LO phonon coupling functions, which are just the oscillating and attenuating functions for spherical Bessel and Neumann functions, in the discussions following, we will only focus on the dispersion relations and the electron-phonon interaction functions $\Gamma_l^{IO,SO}(r)$ for IO and SO phonon modes in the systems. The material parameters are listed in Table I.

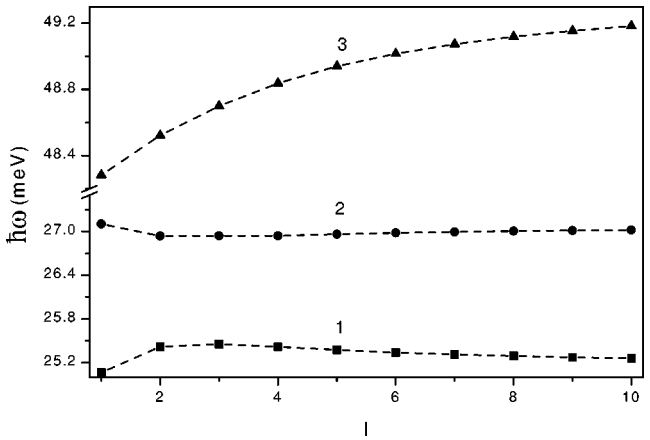

FIG. 2. Dispersion curves of the IO and SO phonon modes for the QDQW with thicknesses 2.35 nm/4.35 nm/∞.

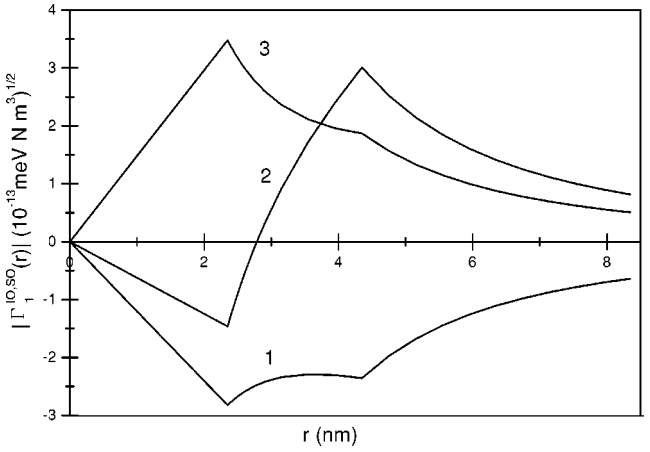

FIG. 3. The coupling functions $\Gamma_1^{IO,SO}(r)$ as a function of r for the QDQW with the same size as that in Fig. 2.

In Fig. 2, the dispersion relations of IO and SO phonon modes are depicted. Contrary to the case of a QWW or QW,[23,24,31–35] in which the IO and SO phonon frequencies were the continuum functions of wave vector, the IO and SO phonon frequencies in the QDQW systems are the discrete spectra for quantum number l. For a certain l, there have only three branches of IO or SO phonon frequencies, which means that Eq. (29) just has three solutions for ω. It should be noted that the frequencies of two branches of modes 1 and 2 are between the longitudinal-optical phonon frequency and the transverse-optical phonon frequency of HgS, and the frequency of the last branch of mode 3 is between those of CdS. Detailed calculations reveal that, with the increase of l, the frequencies of mode 1 and mode 3 approach 25.13 meV and 49.46 meV, respectively. These two values are just the frequency values of IO phonons in a single HgS/CdS spherical heterostructure, and they can be computed by the equation $\varepsilon_1(\omega)/\varepsilon_2(\omega) = -1 - 1/l$.[29] The features of modes 1 and 3 are explained as follows: with increasing l, the potential functions of IO or SO phonon modes became sharper and sharper, and they tend to be localized at a certain interface or surface, which can be seen obviously when comparing Fig. 3 with Fig. 4, so the dispersion frequencies approach the frequency value of single CdS/HgS heterostructures. Hence, modes 1 and 3 can be treated as interface modes. Mode 2 is mainly localized at surface which is more obvious for larger l, and it can be seen clearly in Fig. 4 and Fig. 6 below.

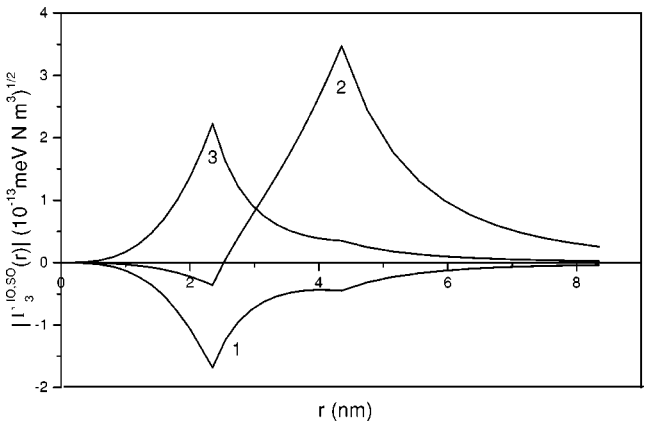

FIG. 4. The coupling functions $\Gamma_3^{IO,SO}(r)$ versus r for the QDQW with the same size as that in Fig. 2.

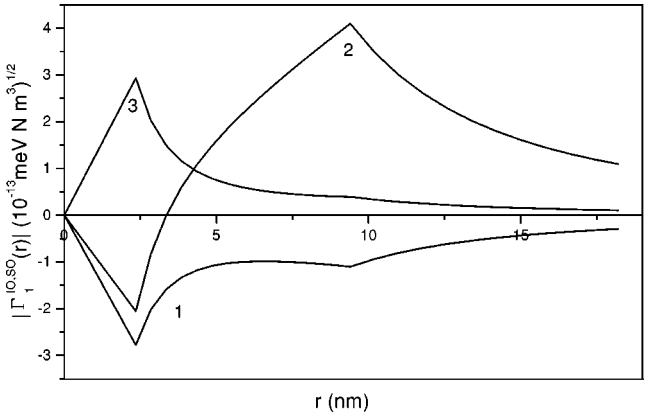

FIG. 5. The coupling functions $\Gamma_1^{IO,SO}(r)$ versus r for the QDQW with thicknesses 2.35 nm/9.4 nm/∞.

In Fig. 3, when $l=1$, the electron-IO or -SO phonon coupling functions $\Gamma_l^{IO,SO}(r)$, as a function of r, are plotted, and the thicknesses of the CdS/HgS/H_2O system are 2.35 nm/4.35 nm/∞. With the same structure as that in Fig. 3, for $l=3$, $\Gamma_l^{IO,SO}(r)$, as a function of r, is presented in Fig. 4. From Fig. 3, it can be observed that, when $l=1$, the distributions of IO or SO phonon potentials on each interface and surface are comparatively average. Comparing Fig. 3 with Fig. 4, we observe, when l increases from 1 to 3, modes 1 and 3 tend to be localized at the interface $r=2.35$ nm, while mode 2 tends to be localized at the surface. In Fig. 5, when the thicknesses of the system are 2.35 nm/9.4 nm/∞, we have drawn the curves of $\Gamma_l^{IO,SO}(r)$ versus r for $l=1$. Comparing the potentials in Fig. 3 with those in Fig. 5, it is found that the increasing of thickness of the spherical shell also makes the distributions of phonon potentials tend to be localized at a certain interface or surface. The observation in Fig. 3–Fig. 5 is easy to be understood. The bigger l and larger shell

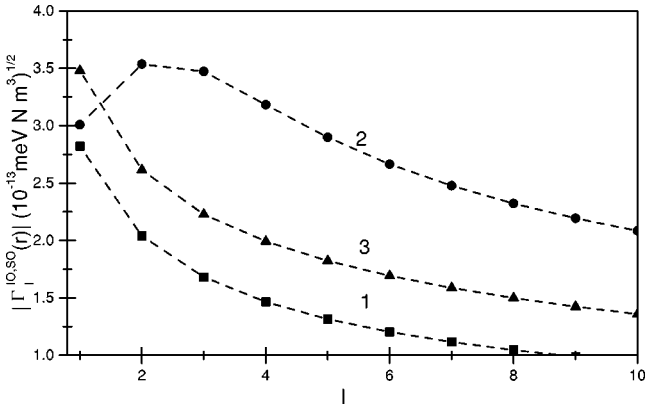

FIG. 6. Absolute values $|\Gamma_l^{IO,SO}(r)|$ as functions of quantum number l for the QDQW system with same structure as that in Fig. 2.

width r_s make the potentials of IO or SO phonons more decoupled on each interface or surface, and in the limiting case of l and $r_s \to \infty$, each IO or SO phonon mode is completely decoupled. The results may be helpful to study and comprehend the polaron effect, electron scattering, etc., in the systems.

In Fig. 6, we show the absolute values $|\Gamma_l^{IO,SO}(r)|$ as a function of quantum number l for the same structure as in Fig. 3. Via the analysis in Fig. 3–Fig. 5, we have chosen $r = 2.35$ nm for modes 1 and 3, and $r = 4.35$ nm for mode 2. From the figure, it can be seen that the functions $|\Gamma_l^{IO,SO}(r)|$ are monotonic attenuating functions when $l \geqslant 2$, and the surface mode 2 plays an important role in the electron-IO and SO interaction. -So, in the case of weak coupling, it is convenient to use perturbation method to investigate the polaronic effect in the QDQW system, which is our sequential research project.

IV. SUMMARY

In the present paper, we have investigated phonon modes in a QDQW with a central core and a layer of shell material in the nonpolar dielectric surrounding medium within the DC approximation. A proper eigenfunction for LO1 modes is adopted and a legitimate eigenfunction for LO2 modes is constructed. The orthogonal relations of the polarization vector for LO phonon modes and IO or SO phonon modes are obtained. The expressions of the confined LO and IO or SO phonon modes, the dispersion relations of the IO and SO phonons, operators for the phonon fields, and corresponding Fröhlich electron-phonon interaction Hamiltonians are also derived. Numeral computations on a HgS/CdS QDQW are performed for the dispersion relations and the electron-phonon interaction functions for IO and SO phonon modes in the systems. The main results are the following:

(i) In the system, there exists three branches of IO or SO phonon modes, and two frequencies of theirs are between $\omega_{LO,\mathrm{HgS}}$ and $\omega_{TO,\mathrm{HgS}}$, and one is between $\omega_{LO,\mathrm{CdS}}$ and $\omega_{TO,\mathrm{CdS}}$. With increasing quantum number l, the frequencies of two modes approach that of the single HgS/CdS heterostructure, for the features of the phonon modes, and a reasonable explanation has been given.

(ii) For the small quantum number l and the thin thickness of the spherical shell r_s, the distributions of the IO and SO phonon potential on each interface and surface are comparatively average. With increasing l and r_s, the distributions of the potential tend to be localized at a certain interface or surface. Detailed study reveals that the electron-SO phonon coupling is more significant.

It is obvious that the theoretical scheme described in this paper applies to the QDQW systems with multiple shell wells provided the conditions of long phonon wavelength are satisfied.[31] We hope this paper will stimulate more theoretical and experimental work, which could be helpful for the study of the influence of phonons on physical properties in QDQW systems.

ACKNOWLEDGMENTS

This work is supported by Guangdong Provincial Natural Science Foundation of China.

APPENDIX

Now, we prove that $T_l(a_{ln}r/r_c)$ and $T_l(a_{lm}r/r_c)$ are orthogonalized within the range of $r_c \leqslant r \leqslant r_s$. Via the definition of $T_l(a_{ln}r/r_c)$, Eq. (14), it can be seen that $T_l(a_{ln}r/r_c)$ and $T_l(a_{lm}r/r_c)$ satisfy the spherical Bessel equations

$$r^2 \frac{d^2 T_l(a_{ln}r/r_c)}{dr^2} + 2r \frac{dT_l(a_{ln}r/r_c)}{dr} + \left[\frac{a_{ln}^2}{r_c^2} r^2 - l(l+1) \right] T_l(a_{ln}r/r_c) = 0, \quad \text{(A1)}$$

$$r^2 \frac{d^2 T_l(a_{lm}r/r_c)}{dr^2} + 2r \frac{dT_l(a_{lm}r/r_c)}{dr} + \left[\frac{a_{lm}^2}{r_c^2} r^2 - l(l+1) \right] T_l(a_{lm}r/r_c) = 0. \quad \text{(A2)}$$

Using Eq. (A1) $\times T_l(a_{lm}r/r_c) -$ Eq. (A2) $\times T_l(a_{ln}r/r_c)$, we get

$$\begin{aligned} r^2 \left(\frac{a_{ln}^2}{r_c^2} - \frac{a_{lm}^2}{r_c^2} \right) & T_l(a_{ln}r/r_c) T_l(a_{lm}r/r_c) \\ &= r^2 \left[\frac{d^2 T_l(a_{lm}r/r_c)}{dr^2} T_l(a_{ln}r/r_c) - \frac{d^2 T_l(a_{ln}r/r_c)}{dr^2} T_l(a_{lm}r/r_c) \right] \\ &\quad + 2r \left[\frac{dT_l(a_{lm}r/r_c)}{dr} T_l(a_{ln}r/r_c) - \frac{dT_l(a_{ln}r/r_c)}{dr} T_l(a_{lm}r/r_c) \right] \\ &= \frac{d}{dr} \left\{ r^2 \left[\frac{dT_l(a_{lm}r/r_c)}{dr} T_l(a_{ln}r/r_c) - \frac{dT_l(a_{ln}r/r_c)}{dr} T_l(a_{lm}r/r_c) \right] \right\}. \end{aligned} \quad \text{(A3)}$$

Integrating both sides of Eq. (A3) from r_c to r_s yields

$$\left(\frac{a_{ln}^2}{r_c^2}-\frac{a_{lm}^2}{r_c^2}\right)\int_{r_c}^{r_s} r^2 T_l(a_{ln}r/r_c)T_l(a_{lm}r/r_c)dr$$
$$=\left\{r^2\left[\frac{dT_l(a_{lm}r/r_c)}{dr}T_l(a_{ln}r/r_c)-\frac{dT_l(a_{ln}r/r_c)}{dr}T_l(a_{lm}r/r_c)\right]\right\}_{r_c}^{r_s}\equiv 0. \quad \text{(A4)}$$

We have made use of the boundary condition at $r=r_c$ and $r=r_s$ [Eq. (15)]. Via Eq. (A4), we get

$$\int_{r_c}^{r_s} T_l(a_{ln}r/r_c)T_l(a_{lm}r/r_c)r^2dr^2=N\delta_{nm}, \quad \text{(A5)}$$

where N is a certain constant. So $T_l(a_{ln}r/r_c)$ and $T_l(a_{lm}r/r_c)$ are orthogonalized within the range $r_c\leqslant r\leqslant r_s$.

*Corresponding author. Mailing address: Department of Physics, Guihuagang Campus, Guangzhou University, Guangzhou 510405, P. R. China. Email address: zhangli-gz@263.net

[1] A. Mews, A. Eychmüller, M. Giersig, D. Schooss, and H. Weller, J. Phys. Chem. **98**, 934 (1994).
[2] A. Eychmüller, A. Mews, and H. Weller, Chem. Phys. Lett. **208**, 59 (1993).
[3] A. Eychmüller, T. Vossmeyer, A. Mews, and H. Weller, J. Lumin. **58**, 223 (1994).
[4] Joseph W. Haus, H.S. Zhou, I. Honma, and H. Komiyama, Phys. Rev. B **47**, 1359 (1993).
[5] D. Schooss, A. Echmüller, and H. Weller, Phys. Rev. B **49**, 17 072 (1994).
[6] Kai Chang and Jian-Bai Xia, Phys. Rev. B **57**, 9780 (1998).
[7] Garnett W. Bryant, Phys. Rev. B **52**, R16 997 (1995).
[8] J.M. Ferreyra and C.R. Proetto, Phys. Rev. B **57**, 9061 (1998).
[9] L. Zhang, H.J. Xie, and C.Y. Chen, Commun. Theor. Phys. **37**, 755 (2002).
[10] Chen Chuan-yu, Li Waisang, and Jin Pei-wan, Commun. Theor. Phys. **28**, 9 (1997).
[11] Hong-Jing Xie, Chuan-Yu Chen, and Ben-Kun Ma, J. Phys.: Condens. Matter **12**, 8623 (2000).
[12] Hong-Jing Xie, Chuan-Yu Chen, and Ben-Kun Ma, Phys. Rev. B **61**, 4827 (2000).
[13] Hong-Jing Xie and Chuan-Yu Chen, Eur. Phys. J. B **5**, 215 (1998).
[14] G.Q. Hai, F.M. Peeters, and J.T. Devreese, Phys. Rev. B **42**, 11 063 (1990).
[15] M.H. Degani and G.A. Farias, Phys. Rev. B **42**, 11 950 (1990).
[16] K.D. Zhu and S.W. Gu, Phys. Lett. A **164**, 465 (1992).
[17] L. Wendler, A.V. Chaplik, R. Haupt, and O. Hipolito, J. Phys.: Condens. Matter **5**, 8031 (1993).
[18] K. Sood, J. Menendez, M. Cardona, and K. Ploog, Phys. Rev. Lett. **54**, 2111 (1985); **54**, 2115 (1985); P. Lambin, J.P. Vigneron, A.A. Lucas, P.A. Thiry, M. Liehr, J.J. Pireaux, R. Caudano, and T.J. Kuech, *ibid.* **56**, 1842 (1986); Klein M.V., IEEE J. Quantum Electron. **QE-22**, 1760 (1986).
[19] R. Fuchs and K.L. Kliewer, Phys. Rev. A **140**, A2076 (1977).
[20] J. Licari and R. Evrard, Phys. Rev. B **15**, 2254 (1965).
[21] L. Wendler, Phys. Status Solidi B **129**, 513 (1985).
[22] L. Wendler and R. Haupt, Phys. Status Solidi B **143**, 487 (1987).
[23] N. Mori and T. Ando, Phys. Rev. B **40**, 6175 (1989).
[24] Shi Jun-jie and Pan Shao-hua, J. Appl. Phys. **80**, 3863 (1996).
[25] S.N. Klimin, E.P. Pokatilov and V.M. Fomin, Phys. Status Solidi B **184**, 373 (1994).
[26] Wai-Sang Li and Chuan-Yu Chen, Physica B **229**, 375 (1997).
[27] M.C. Klein, F. Hache, D. Ricard, and C. Flytzanix, Phys. Rev. B **42**, 11 123 (1990).
[28] E. Roca, C. Trallero-Giner, M. Cardona, Phys. Rev. B **49**, 13 704 (1994).
[29] R.M. de la Cruz, Teitsworth, M.A. Stroscio, Phys. Rev. B **52**, 1489 (1995).
[30] M. Tkach, V. Holovatsky, O. Voitsekhivska, and M. Mikhalyova, Phys. Status Solidi B **203**, 373 (1997).
[31] Kun Huang and Bangfen Zhu, Phys. Rev. B **38**, 13 377 (1988).
[32] P.A. Knipp and T.L. Reinecke, Phys. Rev. B **46**, 10 310 (1992).
[33] H. Rücker, E. Molinari, and P. Lugli, Phys. Rev. B **45**, 6747 (1992).
[34] Ph. Lambin, P. Senet, and A.A. Lucas, Phys. Rev. B **44**, 6416 (1991).
[35] R. Enderlein, Phys. Rev. B **43**, 14 513 (1991).